J Neurophysiol 93: 1111–1118, 2005.
First published September 22, 2004; doi:10.1152/jn.00658.2004.

Report

Slow Adaptation in Fast-Spiking Neurons of Visual Cortex

V. F. Descalzo,[1] L. G. Nowak,[2] J. C. Brumberg,[2,3] D. A. McCormick,[2] and M. V. Sanchez-Vives[1,2]

[1]*Instituto de Neurociencias, Universidad Miguel Hernández-CSIC, San Juan de Alicante, Spain;* [2]*Department of Neurobiology, Yale University, New Haven, Connecticut; and* [3]*Department of Psychology, Queens College, City University of New York, Flushing, New York*

Submitted 30 June 2004; accepted in final form 6 September 2004

Descalzo, V. F., L. G. Nowak, J. C. Brumberg, D. A. McCormick, and M. V. Sanchez-Vives. Slow adaptation in fast-spiking neurons of visual cortex. *J Neurophysiol* 93: 1111–1118, 2005. First published September 22, 2004; doi:10.1152/jn.00658.2004. Fast-spiking (FS) neurons are a class of inhibitory interneurons classically characterized as having short-duration action potentials (<0.5 ms at half height) and displaying little to no spike-frequency adaptation during short (<500 ms) depolarizing current pulses. As a consequence, the resulting injected current intensity versus firing frequency relationship is typically steep, and they can achieve firing frequencies of ≤1 kHz. Here we have investigated the properties of FS neurons discharges on a longer time scale. Twenty second discharges were induced in electrophysiologically identified FS neurons by means of current injection either with sinusoidal current or with square pulses. We found that virtually all FS neurons recorded in cortical slices do show spike-frequency adaptation but with a slow time course (τ = 2–19 s). This slow time course has precluded the observation of this property in previous studies that used shorter pulses. Contrary to the classical view of FS neurons functional properties, long-duration discharges were followed by a slow afterhyperpolarization lasting ≤23 s. During this postadaptation period, the excitability of the neurons was decreased on average for 16.7 ± 6.8 s, therefore rendering the cell less responsive to subsequent afferent inputs. Slow adaptation is also reported here for FS neurons recorded in vivo. This longer time scale of adaptation in FS neurons may be critical for balancing excitation and inhibition as well as for the understanding of cortical network computations.

INTRODUCTION

Fast-spiking (FS) neurons are an electrophysiologically defined subtype of cortical neuron that corresponds to several morphological subtypes of non-pyramidal cells in the hippocampus and cortex (Kawaguchi and Kubota 1993, 1997; McCormick et al. 1985; Tasker et al. 1996; Thomson et al. 1996). Classically, cortical neurons have been classified as FS based on their short-duration action potentials (<0.5 ms spike width at half-amplitude), rapid rate of spike repolarization, lack of spike-frequency adaptation, and a steep frequency versus injected current relationship (McCormick et al. 1985; Nowak et al. 2003). The lack of repetitive burst firing in FS neurons differentiates this cell class from another type neuron, chattering cells, that display equally fast action potentials but generate them in bursts (Brumberg et al. 2000; Gray and McCormick 1996; Nowak et al. 2003). FS neurons can discharge at high rates, sometimes reaching 1 kHz, and they have a steep frequency versus injected current relationship. These properties have been characterized in the cortex in vitro (Connors and Gutnick 1990; Galarreta and Hestrin 2001; Kawaguchi 1993; Llinas et al. 1991; McCormick et al. 1985; Thomson et al. 1996) and in vivo (Azouz et al. 1997; Contreras and Palmer 2003; Mountcastle et al. 1969; Nowak et al. 2003; Nunez et al. 1993; Simons 1978). A significant point of agreement between the in vivo and in vitro studies is that FS neurons can discharge action potentials at high rates with little or no spike frequency adaptation or attenuation in spike height. The basis for some of these functional properties have been traced to the molecular level, and they are attributable to the expression of specific Na^+ and K^+ channels that are characterized by fast activation and recovery from inactivation kinetics (Martina and Jonas 1997; Rudy and McBain 2001). The rising phase of Na^+ channel activation in FS and regular-spiking neurons are governed by similar kinetics, but the rate in which the Na^+ channels recover from inactivation is faster in FS neurons, thus allowing them to generate subsequent action potentials sooner (Martina and Jonas 1997). In a synergistic arrangement, FS neurons express K^+ channels of the Kv3 family that mediate a very fast repolarization, therefore shortening the action potential duration and facilitating recovery from Na^+ channel inactivation (Erisir et al. 1999; McBain and Fisahn 2001; Rudy and McBain 2001; Rudy et al. 1999).

In the present report, we show that the presence or absence of spike-frequency adaptation in FS neurons is dependent on the length of time they are stimulated. For short-duration stimuli (e.g., <500-ms depolarizing current pulses), FS neurons show little or no spike-frequency adaptation. However, we find that, although they do not show adaptation with short pulses, FS neurons do display adaptation during long (~20 s) periods of activation. Additionally, this prolonged activation evokes a slow afterhyperpolarization (AHP) that decreases excitability for tens of seconds. Slow adaptation and AHPs of this time scale have been previously described for cortical pyramidal neurons, the underlying current being a Na^+-dependent K^+ current (Constanti and Sim 1987; Kubota and Saito 1991; Safronov and Vogel 1996; Sanchez-Vives et al. 2000b; Schwindt et al. 1989). This current has been implicated in vivo as one of the cellular mechanisms that underlie the phenomenon of contrast adaptation (Sanchez-Vives et al. 2000a,b). The finding that slow frequency adaptation also occurs in FS neurons may have important implications for understanding the computations performed by the cortical network.

METHODS

In vitro experiments were performed on cortical slices from 2- to 6-mo-old ferrets of either sex that were deeply anesthetized with

Address for reprint requests and other correspondence: M. V. Sanchez-Vives, Instituto de Neurociencias, Universidad Miguel Hernández-CSIC, Apartado 18. 03550 San Juan de Alicante, Spain. (E-mail: mavi.sanchez@umh.es).

The costs of publication of this article were defrayed in part by the payment of page charges. The article must therefore be hereby marked "*advertisement*" in accordance with 18 U.S.C. Section 1734 solely to indicate this fact.

pentobarbital sodium (40 mg/kg) and decapitated. Their brains were quickly removed and placed in ice-cold cutting solution (see following text). Ferrets were cared for and used in accordance with all appropriate regulatory guidelines. Four hundred-micrometer-thick coronal slices of the primary visual cortex were cut on a vibratome. A modification of the technique developed by Aghajanian and Rasmussen (1989) was used to increase tissue viability. After preparation, slices were placed in an interface-style recording chamber (Fine Sciences Tools, Foster City, CA) and bathed in artificial cerebrospinal fluid (ACSF) containing (in mM) 124 NaCl, 2.5 KCl, 2 $MgSO_4$, 1.25 $NaHPO_4$, 2 $CaCl_2$, 26 $NaHCO_3$, and 10 dextrose and was aerated with 95% O_2-5% CO_2 to a final pH of 7.4. Bath temperature was maintained at 34–35°C. Intracellular recordings were initiated after 2 h of recovery. Sharp intracellular recording electrodes were formed on a Sutter Instruments (Novato, CA) P-80 micropipette puller from medium-walled glass and beveled on a Sutter Instruments beveller to final resistances of 50–100 MΩ. Micropipettes were filled with 2 M KAc. Recordings were digitized, acquired and analyzed using a data-acquisition interface and software from Cambridge Electronic Design (Cambridge, UK).

Intracellular recordings in vivo were obtained in the primary visual cortex of cats following the methodology that we have previously described (Sanchez-Vives et al., 2000a). In short, adult cats were anesthetized with ketamine (12–15 mg/kg im) and xylazine (1 mg/kg im). The cat was then mounted in a stereotaxic frame and ventilated with either a mixture of nitrous oxide and oxygen 2:1 with halothane (1.5%), or with oxygen and isoflurane (2.5%). A craniotomy (3–4 mm wide) was made overlying the representation of the area centralis of area 17. During recording, anesthesia was maintained with 0.4–1% halothane or with 0.5–2% isoflurane. The heart rate, expiratory CO_2 concentration, rectal temperature, and blood O_2 concentration were monitored throughout the experiment and maintained at 150–180 bpm, 3–4%, 37–38°C, and >95%, respectively. The electroencephalogram (EEG) and the absence of reaction to noxious stimuli were regularly checked to ensure an adequate depth of anesthesia. To minimize pulsation arising from the heartbeat and respiration, a cisternal drainage and a bilateral pneumothorax were performed, and the animal was suspended by the rib cage to the stereotaxic frame. After the recording session, the animal was given a lethal injection of pentobarbital sodium. This protocol was approved by the Yale University Institutional Animal Care and Use Committees and conforms to the guidelines recommended in *Preparation and Maintenance of Higher Mammals During Neuroscience Experiments*, National Institutes of Health Publication No. 91–3207.

Intracellular recordings were obtained with identical micropipettes to the ones used to record from the cortical slices. Data recording and acquisition were made using the same methods as for the in vitro data.

To identify neurons as FS we used 300- to 500-ms depolarizing current pulses. Longer periods of firing were induced by sinusoidal current injection at a frequency of 2 Hz for 20 s or by depolarizing square pulses of 20 s. The instantaneous frequency was computed as the inverse of the interspike interval. Responses to several repetitions of the current injection were averaged, and they were quantified as spikes per cycle for sinusoidal current injections or in spikes per second for the square pulse current injections (500-ms bins). The slow spike frequency adaptation was measured as the firing rate decay between the first and the last 500 ms of the 20 s of stimulation. The decay time constant was determined by fitting an exponential to the 40 values corresponding to the average number of spikes per cycle (sinusoids) or to the mean frequency for 500-ms bins (square pulse; Fig. 1, *E* and *G*). To minimize the effects of the synaptic noise in vivo, the adaptation strength in vivo was determined from the amplitude at *time 0* and 20 s given by the exponential function. Postadaptation excitability change was assayed by injecting depolarizing current pulses (120–300 ms). Data are reported as means ± SD.

RESULTS

Fifteen FS neurons recorded from slices of ferret visual cortex were included in this study. To be included, the neurons fulfilled the following criteria (McCormick et al. 1985; Nowak et al. 2003): short-duration action potentials (0.35 ± 0.06 ms), absence of burstiness, little or no spike-frequency adaptation during <500-ms depolarizing pulses, and a steep relationship of the intensity of current injection versus the frequency of the discharge. Figure 1 (*A–D*) illustrates all these properties. The lack of spike frequency adaptation during 300-ms depolarizing pulses regardless of current intensity is manifest in Fig. 1*D*. However, when in the same neuron longer spike trains were induced by means of a prolonged depolarizing pulse (20 s, Fig. 1, *E* and *F*) or sinusoidal current injection (Fig. 1, *G* and *H*), a slow spike-frequency adaptation was revealed. In both cases, the adaptation time constant was 2 s and resulted in a 76% decrease in the firing frequency for the square pulse and of 48% for the sinusoidal current injection.

In our in vitro population data, all the cells (n = 15) showed some degree of slow adaptation after 20 s of high-frequency firing. Slow frequency adaptation was studied in detail in 12 of 15 cells with sinusoidal current injection at 2 Hz. The average decay in the number of spikes per cycle was of 44.0 ± 15.8%, and the average time constant of this decay was 8.8 ± 5.8 s (n = 12). Slow frequency adaptation was also explored by injecting 20-s duration pulses in 5 of 15 neurons (Fig. 1, *E* and *F*). The average firing rate decay during 20-s depolarizing pulses was 53.5 ± 30.7% (last 0.5 s with respect to the 1st 0.5 s) and the time constant of the decay was 6.7 ± 3.3 s.

A slow AHP of the membrane potential was observed following the high-frequency discharge induced using either protocol (Figs. 1, *E* and *G,* and Fig. 2*A*). This slow AHP had an amplitude that varied between 0.7 and 10 mV (5.5 ± 2.7 mV) and was long-lasting, between 3 and 23 s (12.4 ± 5.6 s; n = 11 cells in which the characteristics of the protocol allowed AHP quantification). A significant linear relationship

FIG. 1. Slow frequency adaptation in a fast-spiking (FS) neuron recorded in vitro. *A*: spike-triggered average of the action potential (*top*). *Bottom*: the 1st derivative shows the fast rate of depolarization and repolarization characteristic of FS neurons. *B*: the interspike interval (ISI) histogram reveals the lack of burstiness and short ISIs. *C*: current intensity—firing frequency relationship. Each current intensity was applied twice and the responses have been averaged. The SE is displayed in error bars, although in some cases, the SE is too small to be seen. *D*: instantaneous frequency (*top*) and spike discharge (*middle*) in response to the injection of 4 square current pulses of 300-ms duration and increasing intensity (*bottom*). Note that there is no spike-frequency adaptation but a slight acceleration of the discharge during the duration of the current pulse. *E*: response of the same cell to the injection of a long duration (20 s) square pulse of 0.75 nA. The rate of discharge (*top*) is represented in bins of 500 ms, and the voltage trace (*middle*) shows the action potential discharge. Note that spike frequency adaptation develops slowly. *F*: expanded traces of the voltage recording showed in *E,* corresponding to the beginning (*a*), middle (*b*), and end (*c*) of the long-duration (20 s) pulse. *G*: response of the same neuron to sinusoidal current (2-Hz, 1.1-nA peak-to-peak amplitude) injection for 20 s. The slow adaptation of the number of spikes/cycle (*top*) had a time constant of 2.1 s. Afterhyperpolarization (AHP) amplitude: 8 mV; AHP duration: 10–14 s. *H*: expanded traces of the voltage recording depicted in *G,* corresponding to the beginning (*a*) and end (*b*) of the 20-s sinusoidal injection.

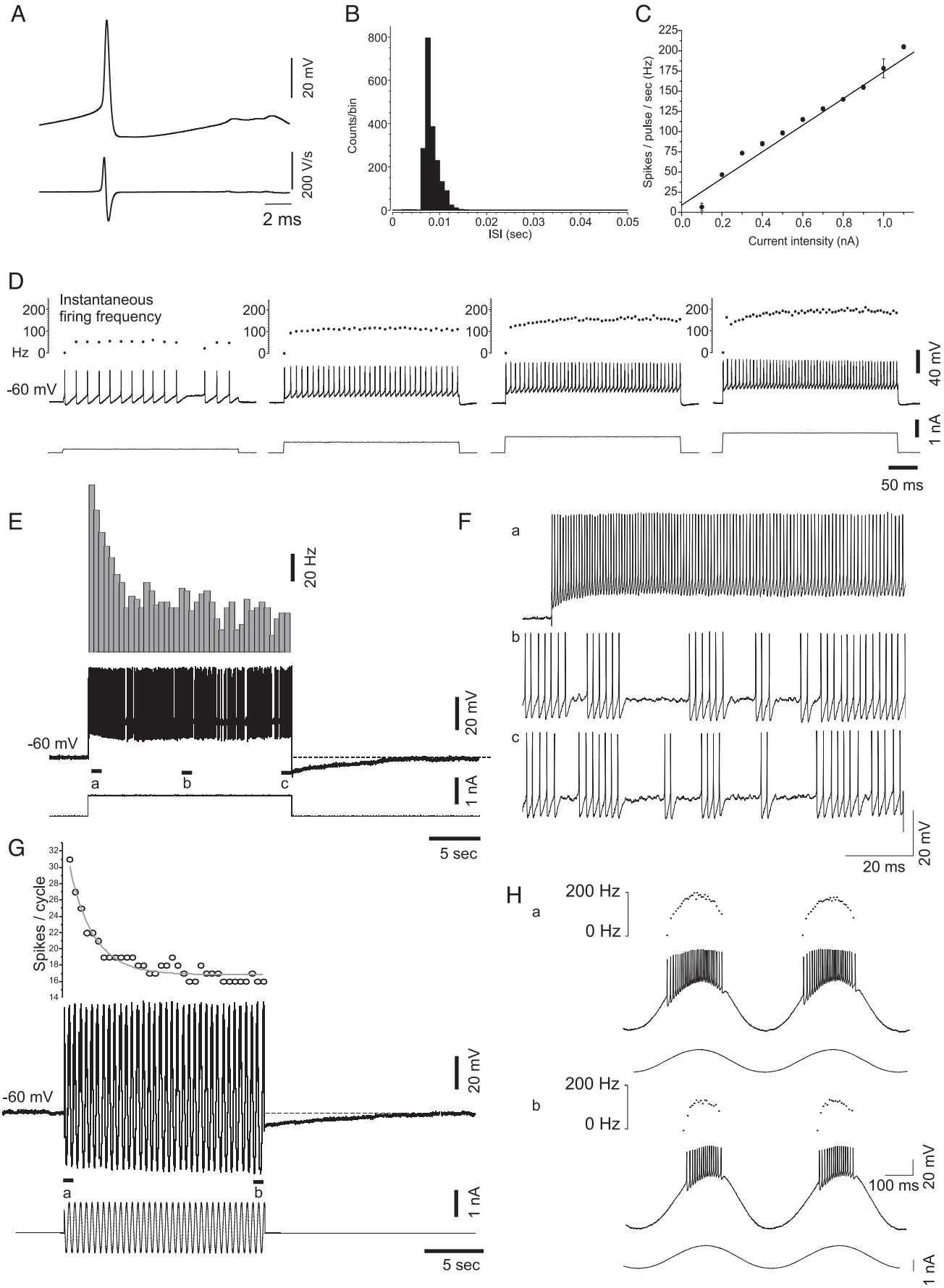

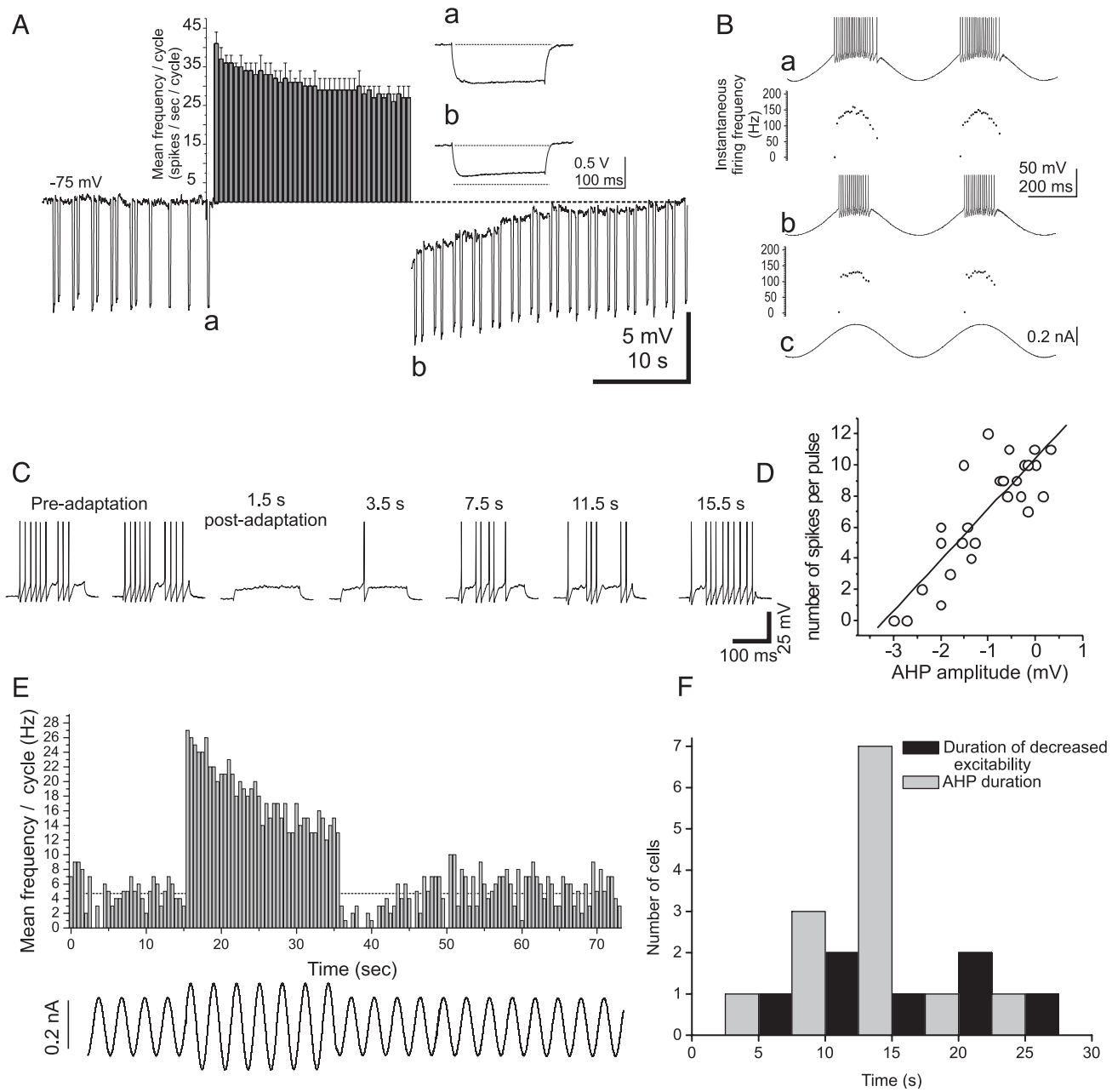

FIG. 2. AHP and decreased excitability following prolonged firing in a representative FS neuron recorded in vitro. *A*: slow AHP (4.6-mV amplitude) following a spike discharge induced by 20 s of sinusoidal current injection (average of 2 trials). Hyperpolarizing pulses (−0.25 nA, 200 ms) were given to test changes in input resistance. Note the decrease in input resistance following the current injection (compare traces *a* and *b*). The peristimulus time histographs (PSTH) plots the mean frequency of the firing calculated with a bin width (0.5 s) equal to the sinewave period. The mean and SD for 2 trials are plotted. *B*: the response of the neuron illustrated in *A* to the 1st (*Ba, top trace*) and last (*Bb, top trace*) cycles of the injected sinewave. Note the decrease in number of spikes/cycle. Below the traces are the instantaneous spike discharge frequency and the injected current trace (*Bc*). *C*: the excitability before and after high-frequency firing (induced as in *A*) was explored by injecting depolarizing pulses of 0.2 nA and 200-ms duration at 0.5 Hz. The *1st 2 traces* were obtained prior to the 20-s adaptation protocol, the subsequent pulses correspond to 1.5, 3.5, 7.5, 11.5, and 15.5 s after the end of the high-frequency firing. Note that the excitability took >10 s to recover. On average this neuron recovered to its preadapted stage in 22.7 ± 8.2 s. *D*: scatter plot representing the amplitude of the AHP preceding the pulses used to test the excitability of the cell (as in *C*) vs. the number of evoked action potentials. AHP was induced by high-frequency firing as in *A*. The linear regression is significant with $P < 0.0001$. Prior high-frequency firing, the number of spikes evoked by the same 0.2-nA pulses was 9.5 ± 1.3. *E*: neuronal discharge for a sinusoidal current injection of low intensity (0.6-nA peak-to-peak amplitude), high intensity (0.9 nA), and low intensity. Mean frequency per cycle (2 Hz) is represented in the PSTH. Note the slow adaptation during the high-frequency firing and long period of postadaptation (firing rate reduction). *Bottom trace*: the current injection protocol, the frequency has been decreased for clarity. *A–E*: correspond to the same neuron. *F*: population histogram of the AHP durations and time of decreased excitability in bins of 5 s.

($P < 0.01$) was found between the duration of the AHP and the time constant of the preceding spike-frequency adaptation (not shown). The slow AHP decreased the excitability of the neurons during the post-discharge period (Fig. 2, *C* and *E*). This decrease in excitability was assessed in seven FS cells by injecting depolarizing current pulses (120–300 ms) before and

following the cessation of the 20-s square pulse or 20 s of sinusoidal current injection. The decrease in excitability lasted for ≤23 s (16.7 ± 6.8 s). Figure 2*D* illustrates the linear relationship between the decrease of the AHP and the recovery of neuronal excitability. The distribution of the values of slow AHP duration and the duration of decreased excitability following a 20 s discharge are represented in Fig. 2*F*.

Intracellular recordings in vivo

The effect of long-lasting current injection has been studied in nine FS neurons recorded intracellularly in cat area 17 in vivo. These cells were classified as FS according to the criteria established by Nowak et al. (2003) (Fig. 3, *A–C*). One of these neurons was previously reported in Sanchez-Vives et al. (2000a). Action potentials were induced by intracellular injection of 2 Hz sinusoidal current during 20 s in eight of these nine neurons (Fig. 3, *F* and *G*). As a result, 62.5% of the neurons ($n = 5/8$) showed slow spike-frequency adaptation. Adaptation strength determined as the firing rate for the last 0.5 s of current injection relative to the firing rate for the first 0.5 s of current injection (see METHODS) was of 29.7 ± 14.0% (range: 10.2 –46.4%). In these five neurons, the average time constant of the firing rate decay was 5.6 ± 4.7 s. No adaptation was observed in the other three FS neurons.

Long-duration (20 s) square depolarizing pulses were injected in three FS neurons (including one that did not receive sinusoidal current injection; Fig. 3*E*). This type of stimulus induced a larger amount of adaptation (40.5 ± 18.8%). In two of the recordings, a single exponential could be fitted to the decay of the firing, the time constants being 2.1 and 5.0 s, respectively.

In two of the six neurons in vivo that showed slow spike-frequency adaptation, a significant reduction in firing rate following the high-frequency firing was observed (note PSTH in Fig. 3*E*). The membrane potential in the remainder cells ($n = 4/6$) was subthreshold in between trials, and changes in the firing following the high-frequency discharge could not be assessed. A slow AHP that followed the high-frequency discharge and may have mediated the reduction in discharge during adaptation and after adaptation could be measured in four of the neurons. The AHP amplitude was between 3 and 8 mV (mean = 5.6 ± 2.7 mV) and the duration between 5 and 10 s (Fig. 3*E, bottom*). The number of FS neurons showing slow AHPs may have been underestimated because the AHP may have been precluded by the large amount of synaptic noise typical of in vivo recordings. In none of the FS neurons that did not exhibit spike-frequency adaptation was there an observable AHP ($n = 3$).

DISCUSSION

FS neurons have been characterized electrophysiologically classically as neurons with fast action potentials, the capability to reach high (≤1 kHz) firing frequencies, steep slopes in discharge frequency versus current intensity relationship, and little or no spike frequency adaptation in response to depolarizing current injection. These characteristics have been established both with in vitro (Connors and Gutnick 1990; McCormick et al. 1985) and in vivo studies (Nowak et al. 2003; Nunez et al. 1993). Here we describe, to our knowledge for the first time, the existence of spike-frequency adaptation in these classically defined FS neurons. In the present study, we demonstrate that neurons with virtually no adaptation in response to short (<0.5 s) depolarizing current pulses, do actually adapt following long (tens of seconds) periods of activation. Both 20-s-long square depolarizing pulses and sinusoidal currents (2 Hz) have been used, and both evoked spike-frequency adaptation. It is important to note that repetitive firing or prolonged activation as utilized in this study may be more relevant to the workings of the brain in vivo, where neurons discharge repetitively in response to external inputs or as part of internal rhythms.

One of the interesting aspects of FS neurons is that they constitute the only electrophysiological cell class unambiguously linked to inhibitory neurons. Neurons with identical or similar electrophysiological properties to those described here, and which have previously been termed FS neurons, have been associated with several subtypes of GABAergic non-pyramidal neurons such as basket and chandelier cells (Azouz et al. 1997; Kawaguchi and Kubota 1993, 1997; McCormick et al. 1985; Thomson and Deuchars 1997); however, in this study, we did not attempt to discern between these various morphological types. It is likely that electrophysiological subtypes exist within the FS category (e.g., see Nowak et al. 2003). For example, one criteria used in some studies is the appearance of an abrupt transition between no action potentials to full trains of action potentials with small increases in the amplitude of injected current pulses (e.g., Kawaguchi and Kubota 1993, 1997). This criteria, however, is not useful for the classifications of in vivo recordings because the presence of background synaptic activity prevents the measurement of threshold behaviors. In this study we have used our quantitative criteria to classify neurons as FS (McCormick et al. 1985; Nowak et al. 2003) with the understanding that this represents a heterogeneous population of cortical GABAergic neurons. In our hands (Azouz et al. 1997; McCormick et al. 1985; Nowak et al. 2003), all of the cells that we have classified as FS neurons and labeled with the same recording methods used here, have been morphologically consistent with what is expected for parvalbumin (+) cells (for a review, see Kawaguchi and Kubota 1997). Parvalbumin (+) cells have been reported to be ≤50% (Gonchar and Burkhalter 1997) (-rat-) and even 74% (van Brederode et al. 1990) (-monkey-) of the total number of inhibitory cells. Therefore the slow adaptation that occurs in at least part of the inhibitory cell population may have a large impact in its associated networks' global discharges.

FS neurons recorded in vitro showed slow frequency adaptation with a time constant in the range of seconds for both sinewave current injections (8.8 ± 5.8 s) and long (20 s) depolarizing pulses (6.7 ± 3.3 s). The reduction of the firing was similar in response to both protocols with an average reduction of ~50% after 20 s. In our previous study on putative excitatory neurons (non-FS neurons; Sanchez-Vives et al. 2000b), we found a very similar reduction of the firing rate (54.7%) at the end of 20 s of sinusoidal current injection. Both adaptation strength and time constant (3.3 s) showed a large heterogeneity between cells (see Fig. 2*C* in Sanchez-Vives et al. 2000b) that could correspond to the inclusion of different cell types such as pyramidal and spiny stellate cells. When compared with the present data, we found that the average

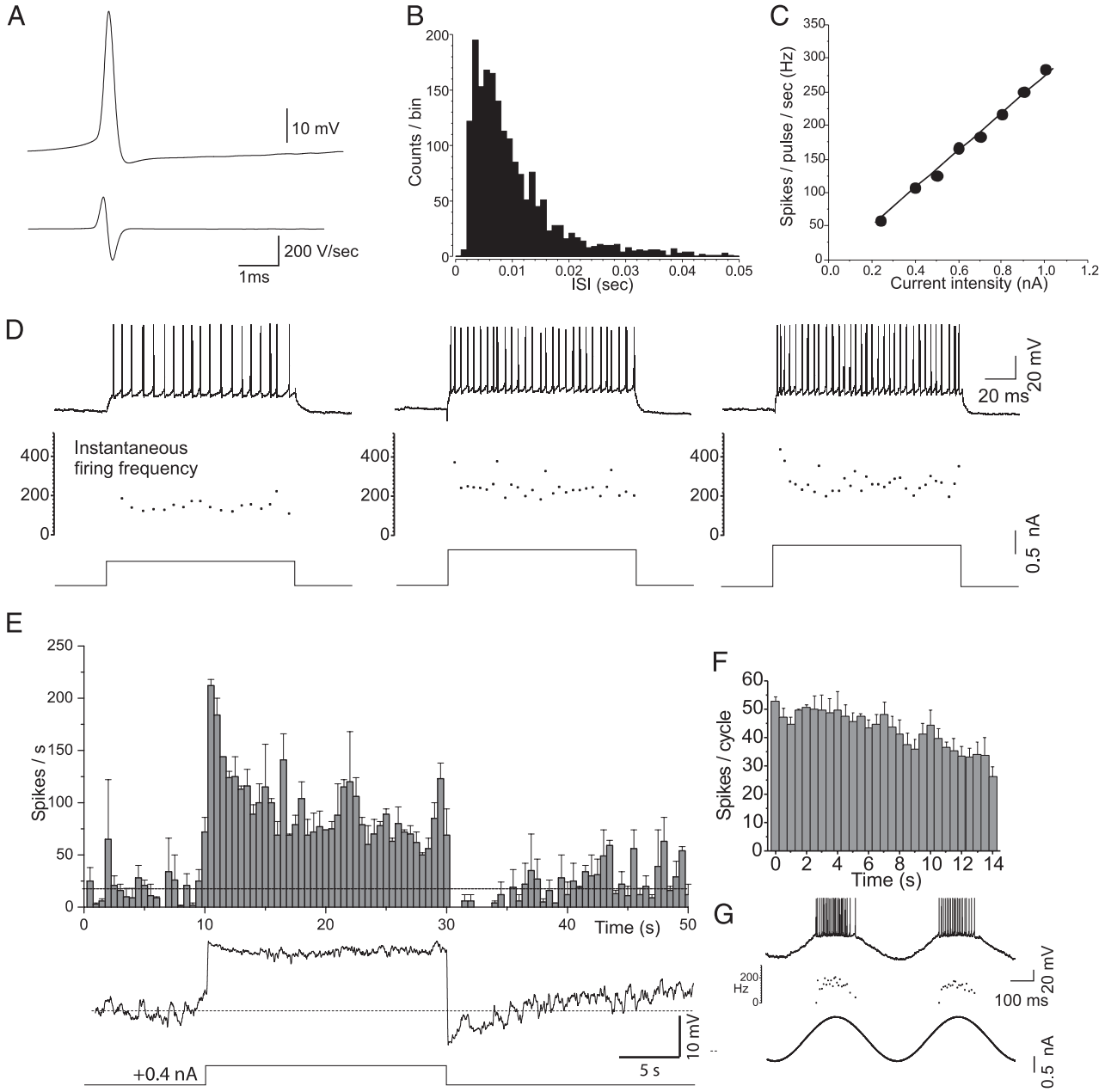

FIG. 3. Slow frequency adaptation in a FS neuron recorded in vivo. *A*: spike-triggered average of the action potential (*top*). *Bottom*: the 1st derivative shows the profile of fast depolarization and repolarization rate characteristic of FS neurons. *B*: interspike interval distribution. Note lack of burstiness and short ISIs. *C*: intensity-frequency relationship (slope = 292 Hz/nA). *D*: voltage response (*top*) to the injection of 3 square current pulses of 300-ms duration and increasing intensity. The instantaneous frequency of the spike discharge is displayed (*middle*). *E*: peristimulus histogram of the same cell to the injection of a long duration (20 s) square pulse of 0.4 nA. The discharge rate is represented in bins of 500 ms, and the error bars correspond to the SE for 2 trials. Note that there is adaptation during the 20 s of firing and a period of decreased spontaneous discharge following the 20-s pulse. The average membrane potential for the same 2 trials is displayed below the PSTH. The voltage trace has been low-pass filtered to eliminate the action potentials and better show the slow AHP that follows the high-frequency firing. *F*: response of the same neuron to sinusoidal current (2 Hz, 0.8-nA peak-to-peak amplitude) injection for 15 s. The histogram displays the average number of spikes/cycle for 3 trials. Error bars represent SE. The time course of the decay did not allow fitting by an exponential curve. *G*: response of the neuron illustrated in *F* to 2 cycles of the injected sinewave. *Top*, membrane voltage; *middle*, instantaneous spike discharge frequency; and *bottom*: the injected current.

decay time constant is significantly faster for non-FS neurons than for FS neurons ($P < 0.0006$). This difference may be due to a relevant role in some of the non-FS neurons of adaptation currents with faster time course such as calcium-dependent potassium currents in non-FS cells (Madison and Nicoll 1984; Pennefather et al. 1985; Schwindt et al. 1992; Vogalis et al. 2003).

Following long (20 s) discharges, FS neurons recorded in vitro displayed a slow AHP that lasted ≤23 s. This AHP was associated with a concurrent decrease in excitability of analogous duration. Therefore the membrane event underlying the slow adaptation in FS neurons appears to be a slow AHP that lasts up to tens of seconds. Furthermore, we find a significant correlation between the time constant of the spike frequency

adaptation and the duration of the subsequent AHP, suggesting that the same mechanism underlies both phenomena. In our study on cortical non-FS neurons (Sanchez-Vives et al. 2000b), we found a slow AHP of 12–75 s following long (20–60 s) discharges that also induced a long-lasting decrease of excitability. In non-FS neurons, we demonstrated that this hyperpolarization was due, at least in large part, to the activation of a K^+ current activated by Na^+ (Sanchez-Vives et al. 2000b). This current has been described in many other neurons (Bader et al. 1985; Bischoff et al. 1998; Dryer et al. 1989; Egan et al. 1992; Foehring et al. 1989; Kim and McCormick 1998; Kubota and Saito 1991; Safronov and Vogel 1996; Schwindt et al. 1989) as well as in heart cells (Kameyama et al. 1984; Luk and Carmeliet 1990). The channels responsible for this current have recently been cloned (Bhattacharjee et al. 2003; Yuan et al. 2003). In the view of the similarity of adaptation and post-adaptation time course, we suggest a Na^+-dependent K^+ current as a plausible candidate to underlie slow adaptation in FS neurons as well. Other possibilities cannot be, however, ruled out. A Na^+/K^+ ATPase electrogenic pump (Gustafson and Wigstrom 1983; Thomas 1972; Thompson and Prince 1986) would yield a similar time course and could contribute to the slow hyperpolarization. This possibility was tested in non-FS neurons (Sanchez-Vives et al. 2000b), where an increase in conductance following activation of the neurons and a lack of blockade by strophandidin argued against an important contribution of a Na^+/K^+ ATPase electrogenic pump.

Although all neurons studied in vitro (15 of 15) displayed slow adaptation, even if small, only 67% of the FS neurons recorded in vivo did. In our in vivo studies, we gave long duration (20 s) stimulus to nine neurons, six of which showed a significant adaptation. Also, the strength of adaptation was less in vivo (30% for the sinusoids, 40% for the pulse) than in vitro (44% for the sinusoids, 53% for the pulse). One explanation for this difference is that we more often used sinusoidal current injections in the in vivo studies, and these are less efficient than long square depolarizing pulses to induce adaptation. Another possibility is that ongoing activity in vivo may have an effect on the steady state of adaptation (Castro-Alamancos 2004): a fraction of Na^+-dependent K^+ current may be activated due to the presence of spontaneous activity in vivo, such that neurons are already partially adapted in the baseline condition. On the other hand, the lack of spontaneous activity in slices would result in neurons that have not been "pre-adapted." This implies that FS neurons in vivo possess the same slow conductance as they do in vitro, but the basal state of their activation may be different in the two instances. Thus a neuron's ability to be in different states of adaptation suggests a mechanism that may allow the neuron to integrate new inputs while still tracking its firing history. Finally, it is reasonable to suggest that adaptation in vitro may be more prominent than in vivo owing to a decrease in efficiency for meeting the metabolic demands of the neurons.

The slow adaptation of a whole population of inhibitory neurons may have important consequences for the computational properties of the cortical network. Neurons in vivo slowly adapt when they are stimulated for extended periods of time, i.e., in response to sustained high contrast stimulation (Albrecht et al. 1984; Carandini and Ferster 1997; Maffei et al. 1973; Movshon and Lennie 1979; Ohzawa et al. 1985; Sanchez-Vives et al. 2000a) or as a result of long-lasting current injection (Sanchez-Vives et al. 2000a). Intrinsic mechanisms such as slow adaptation currents have an effect somewhat similar to recurrent inhibition in the sense that the spike discharge is regulated by the neuron's own previous activity. The fact that both excitatory and inhibitory neurons share similar mechanisms for slow adaptation probably contributes to the excitatory/inhibitory balance within the cortical network (Shu et al. 2003).

ACKNOWLEDGMENTS

Thanks to Dr. R. Gallego for providing laboratory facilities.

GRANTS

This work has been sponsored by Human Frontiers Science Program Organization and Ministerio de Ciencia y Tecnologia (MCYT) to M. V. Sanchez-Vives and by a National Eye Institute grant to D. A. McCormick. V. F. Descalzo was supported by a Formación de Personal Investigator fellowship (MCYT). J. C. Brumberg was supported by National Institute of Mental Health Grants F32MH-12358-01 and MH-01944-01A1.

REFERENCES

Aghajanian GK and Rasmussen K. Intracellular studies in the facial nucleus illustrating a simple new method for obtaining viable motoneurons in adult rat brain slices. *Synapse* 3: 331–338, 1989.

Albrecht DG, Farrar SB, and Hamilton DB. Spatial contrast adaptation characteristics of neurons recorded in the cat's visual cortex. *J Physiol* 347: 713–739, 1984.

Azouz R, Gray CM, Nowak LG, and McCormick DA. Physiological properties of inhibitory interneurons in cat striate cortex. *Cereb Cortex* 7: 534–545, 1997.

Bader CR, Bernheim L, and Bertrand D. Sodium-activated potassium current in cultured avian neurons. *Nature* 317: 540–542, 1985.

Bhattacharjee A, Joiner WJ, Wu M, Yang Y, Sigworth FJ, and Kaczmarek LK. Slick (Slo2.1), a rapidly gating sodium-activated potassium channel inhibited by ATP. *J Neurosci* 23: 11681–11691, 2003.

Bischoff U, Vogel W, and Safronov BV. Na^+-activated K^+ channels in small dorsal root ganglion neurons of rat. *J Physiol* 510: 743–754, 1998.

Brumberg JC, Nowak LG, and McCormick DA. Ionic mechanisms underlying repetitive high-frequency burst firing in supragranular cortical neurons. *J Neurosci* 20: 4829–4843, 2000.

Carandini M and Ferster DA. tonic hyperpolarization underlying contrast adaptation in cat visual cortex. *Science* 276: 949–952, 1997.

Castro-Alamancos MA. Absence of rapid sensory adaptation in neocortex during information processing states. *Neuron* 41: 455–464, 2004.

Connors BW and Gutnick MJ. Intrinsic firing patterns of diverse neocortical neurons. *Trends Neurosci* 13: 99–104, 1990.

Constanti A and Sim JA. Calcium-dependent potassium conductance in guinea pig olfactory cortex neurones in vitro. *J Physiol* 387: 173–194, 1987.

Contreras D and Palmer L. Response to contrast of electrophysiologically defined cell classes in primary visual cortex. *J Neurosci* 23: 6936–6945, 2003.

Dryer SE, Fujii JT, and Martin AR. A Na^+-activated K^+ current in cultured brain stem neurones from chicks. *J Physiol* 410: 283–296, 1989.

Egan TM, Dagan D, Kupper J, and Levitan IB. Na(+)-activated K^+ channels are widely distributed in rat CNS and in *Xenopus* oocytes. *Brain Res* 584: 319–321, 1992.

Erisir A, Lau D, Rudy B, and Leonard CS. Function of specific K(+) channels in sustained high-frequency firing of fast-spiking neocortical interneurons. *J Neurophysiol* 82: 2476–2489, 1999.

Foehring RC, Schwindt PC, and Crill WE. Norepinephrine selectively reduces slow Ca^{2+}- and Na^+-mediated K^+ currents in cat neocortical neurons. *J Neurophysiol* 61: 245–256, 1989.

Galarreta M and Hestrin S. Spike transmission and synchrony detection in networks of GABAergic interneurons. *Science* 292: 2295–2299, 2001.

Gonchar Y and Burkhalter A. Three distinct families of GABAergic neurons in rat visual cortex. *Cereb Cortex* 7: 347–58, 1997.

Gray CM and McCormick DA. Chattering cells: superficial pyramidal neurons contributing to the generation of synchronous oscillations in the visual cortex. *Science* 274: 109–113, 1996.

Gustafsson B and Wigstrom H. Hyperpolarization following long-lasting tetanic activation of hippocampal pyramidal cells. *Brain Res* 275: 159–163, 1983.

Kameyama M, Kakei M, Sato R, Shibasaki T, Matsuda H, and Irisawa H. Intracellular Na^+ activates a K^+ channel in mammalian cardiac cells. *Nature* 309: 354–356, 1984.

Kawaguchi Y. Physiological, morphological, and histochemical characterization of three classes of interneurons in rat neostriatum. *J Neurosci* 13: 4908–4923, 1993.

Kawaguchi Y and Kubota Y. Correlation of physiological subgroupings of nonpyramidal cells with parvalb. *J Neurophysiol* 70: 387–396, 1993.

Kawaguchi Y and Kubota Y. GABAergic cell subtypes and their synaptic connections in rat frontal cortex. *Cereb Cortex* 7: 476–486, 1997.

Kim U and McCormick DA. Functional and ionic properties of a slow afterhyperpolarization in ferret perigeniculate neurons in vitro. *J Neurophysiol* 80: 1222–1235, 1998.

Kubota M and Saito N. Sodium- and calcium-dependent conductances of neurones in the zebra finch hyperstriatum ventrale pars caudale in vitro. *J Physiol* 440: 131–142, 1991.

Llinas RR, Grace AA, and Yarom Y. In vitro neurons in mammalian cortical layer 4 exhibit intrinsic oscillatory activity in the 10- to 50-Hz frequency range. *Proc Natl Acad Sci USA* 88: 897–901, 1991.

Luk HN and Carmeliet E. Na(+)-activated K^+ current in cardiac cells: rectification, open probability, block and role in digitalis toxicity. *Pfluegers* 416: 766–768, 1990.

Madison DV and Nicoll RA. Control of the repetitive discharge of rat CA1 pyramidal neurons in vitro. *J Physiol* 354: 319–331, 1984.

Maffei L, Fiorentini A, and Bisti S. Neural correlate of perceptual adaptation to gratings. *Science* 182: 1036–1038, 1973.

Martina M and Jonas P. Functional differences in Na^+ channel gating between fast-spiking interneurons and principal neurons of rat hippocampus. *J Physiol* 505.3: 593–603, 1997.

McBain CJ and Fisahn A. Interneurons unbound. *Nat Rev Neurosci* 2: 11–23, 2001.

McCormick DA, Connors BW, Lighthall JW, and Prince DA. Comparative electrophysiology of pyramidal and sparsely spiny stellate neurons of the neocortex. *J Neurophysiol* 54: 782–806, 1985.

Mountcastle VB, Talbot WH, Sakata H, and Hyvarinen J. Cortical neuronal mechanisms in flutter-vibration studied in unanesthetized monkeys: neuronal periodicity and frequency discrimination. *J Neurophysiol* 32: 452–484, 1969.

Movshon JA and Lennie P. Pattern-selective adaptation in visual cortical neurones. *Nature* 278: 850–852, 1979.

Nowak LG, Sanchez-Vives MV, and McCormick DA. Influence of low and high frequency inputs on spike timing in visual cortical neurons. *Cereb Cortex* 7: 487–501, 1997.

Nowak LG, Azouz R, Sanchez-Vives MV, Gray CM, and McCormick DA. Electrophysiological classes of cat primary visual cortical neurons *in vivo* as revealed by quantitative analyses. *J Neurophysiol* 89: 1541–1566, 2003.

Nunez A, Amzica F, and Steriade M. Electrophysiology of cat association cortical cells in vivo: intrinsic properties and synaptic responses. *J Neurophysiol* 70: 418–430, 1993.

Ohzawa I, Sclar G, and Freeman RD. Contrast gain control in the cat's visual system. *J Neurophysiol* 54: 651–667, 1985.

Pennefather P, Lancaster B, Adams PR, and Nicoll RA. Two distinct Ca-dependent K currents in bullfrog sympathetic ganglion cells. *Proc Natl Acad Sci USA* 82: 3040–3044, 1985.

Rudy B, Chow A, Lau D, Amarillo Y, Ozaita A, Saganich M, Moreno H, Nadal MS, Hernandez-Pineda R, Hernandez-Cruz A, Erisir A, Leonard C, and Vega-Saenz dM. Contributions of Kv3 channels to neuronal excitability. *Ann N Y Acad Sci* 868: 304–343, 1999.

Rudy B and McBain CJ. Kv3 channels: voltage-gated K^+ channels designed for high-frequency repetitive firing. *Trends Neurosci* 24: 517–526, 2001.

Sah P. Ca^{2+} activated K^+ currents in neurons: types, physiological roles and modulation. *Trends Neurosci* 19: 150–154, 1996.

Safronov BV and Vogel W. Properties and functions of Na(+)-activated K^+ channels in the soma of rat motoneurons. *J Physiol* 497: 727–734, 1996.

Sanchez-Vives MV, Nowak LG, and McCormick DA. Membrane mechanisms underlying contrast adaptation in cat area 17 in vivo. *J Neurosci* 20: 4267–4285, 2000a.

Sanchez-Vives MV, Nowak LG, and McCormick DA. Cellular mechanisms of long-lasting adaptation in visual cortical neurons in vitro. *J Neurosci* 20: 4286–4299, 2000b.

Schwindt PC, Spain WJ, and Crill WE. Calcium-dependent potassium currents in neurons in cat sensorimotor cortex. *J Neurophysiol* 67: 216–226, 1992.

Schwindt PC, Spain WJ, and Crill WE. Long-lasting reduction of excitability by a sodium-dependent potassium current in cat neocortical neurons. *J Neurophysiol* 61: 233–244, 1989.

Shu Y, Hasenstaub A, and McCormick DA. Turning on and off recurrent balanced cortical activity. *Nature* 423: 288–293, 2003.

Simons DJ. Response properties of vibrissa units in rat SI somatosensory neocortex. *J Neurophysiol* 41: 798–820, 1978.

Tasker JG, Hoffman NW, Kim YI, Fisher RS, Peacock WJ, and Dudek FE. Electrical properties of neocortical neurons in slices from children with intractable epilepsy. *J Neurophysiol* 75: 931–939, 1996.

Thomas RC. Electrogenic sodium pump in nerve and muscle cells. *Physiol Rev* 52: 563–594, 1972.

Thompson SM and Prince DA. Activation of electrogenic sodium pump in hippocampal CA1 neurons following glutamate-induced depolarization. *J Neurophysiol* 56: 507–522, 1986.

Thomson AM and Deuchars J. Synaptic interactions in neocortical local circuits: dual intracellular recordings in vitro. *Cereb Cortex* 7: 510–522, 1997.

Thomson AM, West DC, Hahn J, and Deuchars J. Single axon IPSPs elicited in pyramidal cells by three classes of interneurones in slices of rat neocortex. *J Physiol* 496: 81–102, 1996.

van Brederode JF, Mulligan KA, and Hendrickson AE. Calcium-binding proteins as markers for subpopulations of GABAergic neurons in monkey striate cortex. *J Comp Neurol* 298: 1–22, 1990.

Vogalis F, Storm JF, and Lancaster B. SK channels and the varieties of slow after-hyperpolarizations in neurons. *Eur J Neurosci* 18: 3155–3166, 2003.

Yuan A, Santi CM, Wei A, Wang ZW, Pollak K, Nonet M, Kaczmarek L, Crowder CM, and Salkoff L. The sodium-activated potassium channel is encoded by a member of the Slo gene family. *Neuron* 37: 765–773, 2003.